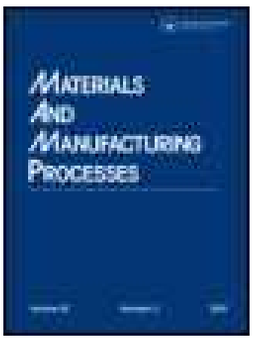

Materials and Manufacturing Processes

ISSN: (Print) (Online) Journal homepage: https://www.tandfonline.com/loi/lmmp20

A novel manufacturing route for integrated 3D-printed composites and cold-sprayed metallic layer

Antonio Viscusi, Roberta Della Gatta, Francesco Delloro, Ilaria Papa, Alessia Serena Perna & Antonello Astarita

To cite this article: Antonio Viscusi, Roberta Della Gatta, Francesco Delloro, Ilaria Papa, Alessia Serena Perna & Antonello Astarita (2021): A novel manufacturing route for integrated 3D-printed composites and cold-sprayed metallic layer, Materials and Manufacturing Processes, DOI: 10.1080/10426914.2021.1942908

To link to this article: https://doi.org/10.1080/10426914.2021.1942908

Published online: 16 Jun 2021.

MATERIALS AND MANUFACTURING PROCESSES
https://doi.org/10.1080/10426914.2021.1942908

A novel manufacturing route for integrated 3D-printed composites and cold-sprayed metallic layer

Antonio Viscusi[a], Roberta Della Gatta[a], Francesco Delloro[b], Ilaria Papa[a], Alessia Serena Perna[a,c], and Antonello Astarita[a]

[a]Department of Chemical, Materials and Industrial Production Engineering, University of Naples Federico II, Naples, Italy; [b]Département Mécanique Et Matériaux, (MINES ParisTech), Paris, France; [c]Department of Management Information and Production Engineering, University of Bergamo, Bergamo, Italy

ABSTRACT

Polymer matrix composites (PMCs) are the most used in aerospace fields due to their special mechanical properties coupled with reduced weight. Metallic structures can be manufactured on the surface of PMCs producing hybrid constructions with intriguing characteristics. The cold spray technology (CS) seems to be the best solution for the manufacturing of metallic coatings on polymer-based substrates. However, the last researches on PMCs metallization through CS were carried out without taking into account a proper manufacturing of the substrates. Therefore, the customized manufacturing of PMCs used as substrates for CS deposition represents a crucial aspect to be considered, the target surface should be designed and manufactured to fit better the CS requirements. In this scenario, the Fused Filament Fabrication method (FFF) is the best solution for tailored composites manufacturing. Therefore, this work aims to develop a novel manufacturing route to produce innovative composite structures by using the FFF technology for the 3D-printed polymer-based substrate and the cold spray technology for the 3D-printed metal deposition. The novelty is that, for the first time, the polymer-based substrates will be designed and manufactured "ad hoc" for the cold spray metallization by using the rapid prototyping 3D-printing process successfully integrated with CS technology.

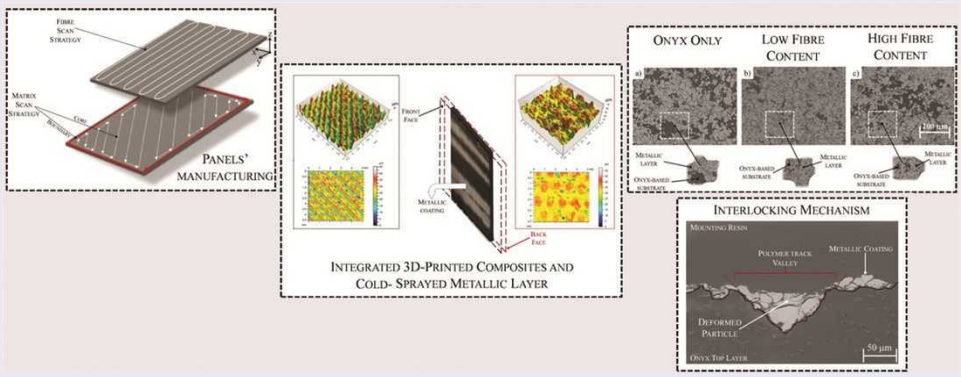

ARTICLE HISTORY
Received 22 January 2021
Accepted 25 May 2021

KEYWORDS
3d-printing; composite; manufacturing; cold; spray; FFF technology; metallization; fibers; coating; coverage; deposition

Introduction

The reinforced polymer matrix composites (PMCs) are vastly used in numerous engineering fields due to their outstanding performances and other unique properties such as ease of formation and machining and good size stability.[1] The main advantages of these materials lie in their anisotropic and heterogeneous properties that allow obtaining low weight – high-performance structures.[2] The use of PMCs in the aerospace field gradually increased in the last years due to the development of new polymers with enhanced mechanical and physical properties.[3,4] However, PMCs field of application could be expanded furtherly if a metallic-based structure (or a Metal Matrix Composite) was manufactured on the polymer-based surface, resulting in a novel hybrid composite structure with intriguing properties. For instance, some of PMCs surface characteristics such as electrical conductivity, thermal conductivity, electromagnetic shielding, erosion, radiation and lightning protection would be improved through the surface metallization process and the coating manufacturing.

Several technologies can be used potentially to metallize the PMCs, such as PVD or CVD,[5,6] electroplating,[7] electroforming,[8] and conventional thermal spraying processes.[9] Unfortunately, these techniques have disadvantages that strongly limit their uses and applications, as reported by Zhou et al..[10] Moreover, some of these technologies may lead the substrate to deterioration and degradation, making the

CONTACT Antonio Viscusi antonio.viscusi@unina.it Department of Chemical, Materials and Industrial Production Engineering, University of Naples Federico II, Piazzale Tecchio 80, Naples, Italy.

metallization impossible to carry out.[11] In this scenario, it is widely accepted in the literature that cold spray technology (CS), a relatively new additive coating technique, is one of the best solutions for the manufacturing of a metallic coating on polymer-based substrates, such as PMCs.[12]

CS technology is a "cold" thermal spray coating technique involving the deposition of micron-sized particles (10–100 μm in diameter[13]) on a target surface. The term cold refers to the capacity of this technique to keep the temperature of the processed powders below the melting point of the particle's material during the deposition process. The result is that the particles impacting the substrate in the solid-state at relatively high velocity deform and bond together for the coating formation and grow-up .[14] That means that CS can be effectively used to spray particles on temperature-sensitive materials, such as polymer matrix composites or plastics without inducing extensive thermal deterioration phenomena, as proved in literature.[15,16] In CS processes, the powders (metallic and/or nonmetallic particles[17]) are dragged by a gas stream (typically air, helium, argon) expanding through a converging-diverging de-Laval nozzle to supersonic conditions.[18] The achieved impact velocities usually range between 300 and 1200 m s^{-1}.[19] As the particles exit from the nozzle at high speeds and impinge on the substrate, they undergo significant plastic deformations and bond to the target surface.[20]

The study of metal particles deposition on composites or polymeric surfaces through the cold spray technology is in its early stage. The first results showed that PMCs metallization's quality is strongly dependent on CS process parameters such as gas species,[11,21] gas pressure and temperature,[11,22] standoff distance[23] and powder typology.[11,24] Moreover, the last researches on this topic proved that the key factors for an effective PMCs metallization are the substrate typology and stratification, which in turn, depend on PMCs manufacturing processes.

In this regard, Gillet et al.[25] suggested that a polymer layer protecting the carbon fibers on top of the substrate seems to be necessary, also finding that the powders deposition depends on the polymer surface layer thickness. Perna et al.[26] studied custom-made composite panels with different matrix thicknesses on the surface to point out the influence of the fibers in the deposition and to study the feasibility and the growth of the coating. Viscusi et al.[27] proposed an original manufacturing method that provides the surface polylactic acid (PLA) treatment for thermosetting basalt fiber-reinforced plastics. So, the issues pointed out by Ganesan et al.[28] for the metallization of thermoset-based materials have been overcome partially.

The last studies on this topic (CS metal depositions on plastics, included composites) were carried out by spraying metallic particles under different working conditions in terms of CS process parameters and substrate typology, without taking account for a proper design and manufacturing of the substrates.[12,25,29,30] In fact, the main outcomes proved that the composite stratification, layup sequence and fiber density, which are strictly related to the composite manufacturing processes, can have a strong influence on the CS deposition process. Therefore, the customized manufacturing of the polymer-based substrates for CS deposition represents a crucial aspect to be considered, namely the target surface should be designed and manufactured to fit better the CS requirements.

For this purpose, there exist different additive manufacturing technologies for composite materials allowing for the production of tailored fiber-reinforced polymer matrix panels.[31] These technologies enable the production of polymer-based components in a single step and, regardless of the complexity of the component, with reduced processing time and cost.[32] In particular, thermoplastic polymers are used thanks to their capacity to be melted and molded even at relatively low temperatures.[33] The most common method for printing a thermoplastic polymer is the Fused Filament Fabrication (FFF) method which relies on the thermal extrusion of a thermoplastic feedstock from a mobile heated nozzle.[34]

FFF technology allows for the deposition of two different types of filaments by using a double extruder. A nozzle is dedicated to a "matrix" filament used to form the outer shell as well as fill the part. The second nozzle takes care of depositing a continuous thread of fiber such as carbon, fiberglass or Kevlar, on each possible layer. The fibers within 3D-printed parts manage to give the polymer-based component a resistance comparable to that of a metal part with lower production cost and a high degree of automation. The reinforcements deposition can be optimized, layer-by-layer, allowing for an increase in design freedom and mechanical performance.[35] Among the several companies developing commercial 3D-printers capable of processing continuous fiber-reinforced composite materials, the Markforged printers excel.

It appears clear that FFF technology, which allows for the manufacturing of customized fiber-reinforced polymer matrix laminates, is a very promising technique to be integrated successfully with the cold spray technology, as it represents the best solution for the manufacturing of 3D-printed panels tailored for the CS requirements.

Therefore, this research work aims to study for the first time in literature a novel manufacturing route for the production of innovative composite structures by using the FFF technology (Markforged) for the 3D-printed polymer-based substrate and the cold spray technology for the 3D-printed metal deposition. For this purpose, both the layup sequence and stratification of the substrates and the cold spray process parameters were varied to study the manufacturing process in its wholeness. Onyx, a novel nylon-based thermoplastic polymer functionalized with short carbon fibers, was chosen as matrix material for the 3D-printed laminates.

Three kinds of laminates were produced and studied as cold-sprayed substrates to evaluate the influence of both the stratification and the fiber percentage: i) Unreinforced Onyx laminates; ii) Onyx reinforced with a continuous carbon fiber deposited alternating one layer of fibers at [0]° and two layers of matrix, and iii) Onyx reinforced with continuous carbon fiber in each layer deposited following the sequence [0/45/90/135]°.

Each laminate was metallized through the Low-Pressure Cold Spray technology (LPCS) by setting the same CS process

parameters. Micron-sized aluminum powders were used for PMCs metallization. The products were sectioned and then observed through optical, SEM and confocal microscopies aiming to analyze the influence of the substrate typology and characteristics on the CS deposition process.

Materials and methods

The 3D-printed composite materials taken into account in this paper were made through the FFF technology (Markforged X7). The used matrix is Onyx, a novel nylon-based material with short carbon fibers dispersed in it. It represents a high strength thermoplastic material, with excellent surface finishing that can be molded unreinforced or reinforced with continuous fibers in order to give a resistance comparable to aluminum. The material provides greater strength and a matte black surface finish to the 3D-printed parts. Compared to traditional nylon, Onyx is about 3.5 times more resistant and has a greater hardness and a HDT (Heat Deflection Temperature) of 140°C .[36] The short carbon fibers dispersed in the nylon filament, modify the behavior of the material on cooling, inducing lower thermal deformations so that the dimensions of the molded pieces faithfully reproduce the model designed in CAD. By selecting printing parameters, such as deposition strategy, and the characteristics of the materials involved, the cloud-based software optimize the process in order to quickly obtain a printout of the desired part.

The dual extruder system generates the composite part, layer-by-layer, according to the Continuous Fiber Fabrication (CFF) process technology. The first nozzle builds the plastic matrix and the second wrap the fiber. With a built-in laser micrometer, the printer automatically scans the processing plate with 1 μm precision to create a contour map of its surface. At this point, it calibrates its measurements with the extrusion readings to correctly set the height of the nozzle and the dynamic adjustment of the topography. In this way, the printer ensures that your printouts are precisely positioned inside the printing chamber (Fig. 1). Given the excellent surface finish obtainable, no further chemical or mechanical processing is required on the molded parts, with a considerable saving in terms of time.

The long carbon fiber used to produce the fiber-reinforced polymers is made up of thin elemental carbon filaments. Fibers have extremely variable chemical and physical properties. The modulus of elasticity varies from about 350 kg/cm^2, a value between the glass fibers and aluminum ones, up to 7000 kg/cm^2, or three times greater than the modulus of steel.[36]

The manufacturing of the specimens was carried out by defining three macro-typologies for the samples, referred now as FO (Full Onyx), LFC (Low Fiber Content) and HFC (High Fiber Content). They are characterized by different fiber volume fractions and layup sequences; in particular:

- FO: Onyx laminates made of nylon, as a thermoplastic matrix, and chopped carbon fibers randomly dispersed in it;
- LFC: Onyx reinforced with a continuous carbon fiber deposited alternating one layer of fibers at [0]° and two layers of matrix;
- HFC: Onyx reinforced with a continuous carbon fiber filament in each layer deposited following the sequence [0/45/90/135]°.

Each panel is 135 mm in length and 36 mm in width. Each layer constituting the stratified panel is about 0.125 mm with a final thickness of the samples equal to t = 4 ± 0.2 mm. For both the reinforced configurations (referred to as LFC and HFC in this activity), the bottom, as well as the top surfaces of the panels,

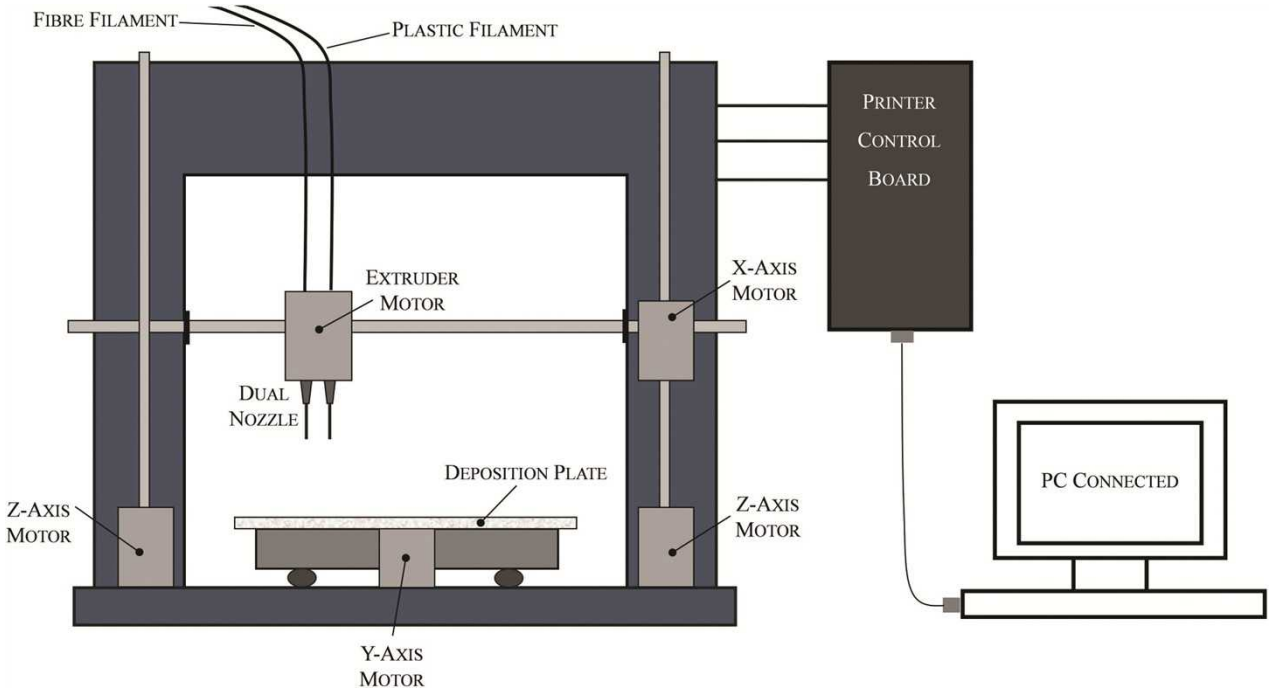

Figure 1. Simple sketch of FFF technology for the 3D-printed polymer-based materials.

were made by depositing four consecutive layers of Onyx matrix. This strategy is used to avoid exposing the fibers on the outer surface and to take advantage of the higher quality surface finish and accuracy ensured by the unreinforced Onyx.

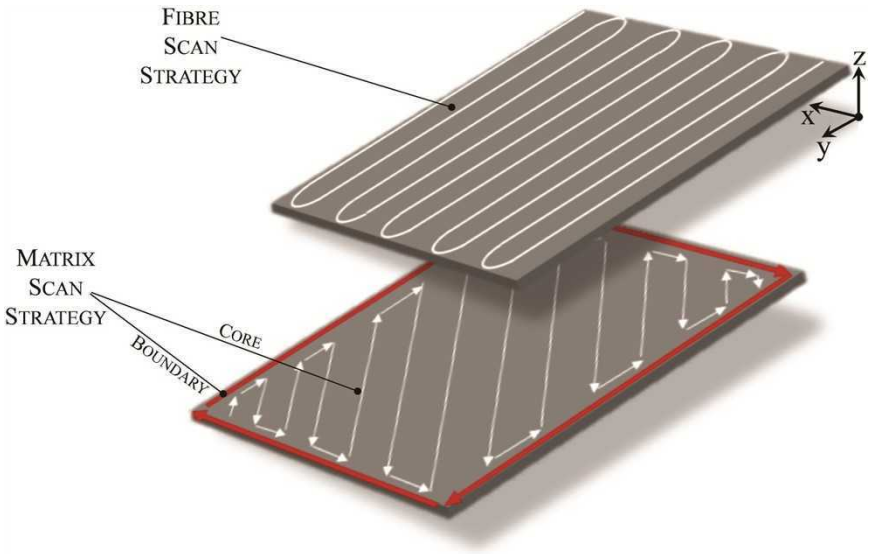

Figure 2. Scan pattern for the panels' manufacturing.

Table 1. Experimental data of the panels' manufacturing. For the "Layup sequence" raw, the subscripted number indicates the number of layers of the same typology. Note that the term "sym" was used to indicate a symmetric configuration.

	FO	LFC	HFC
Matrix Typology	Onyx	Onyx	Onyx
Long carbon fiber layers	NO	YES	YES
Printing temperature [°C]	260	260	260
Layer thickness [mm]	0.125	0.125	0.125
Panel thickness [mm]	4 ± 0.2	4 ± 0.2	4 ± 0.2
Layup sequence	[Onyx $_{16}$] sym	[Onyx $_4$/0°/Onyx $_2$/0°/Onyx $_2$/0°/Onyx $_2$/0°/Onyx $_2$] sym	[Onyx $_4$/(0°/45°/90°/135°)$_3$] sym
Number of layers	32	32	32

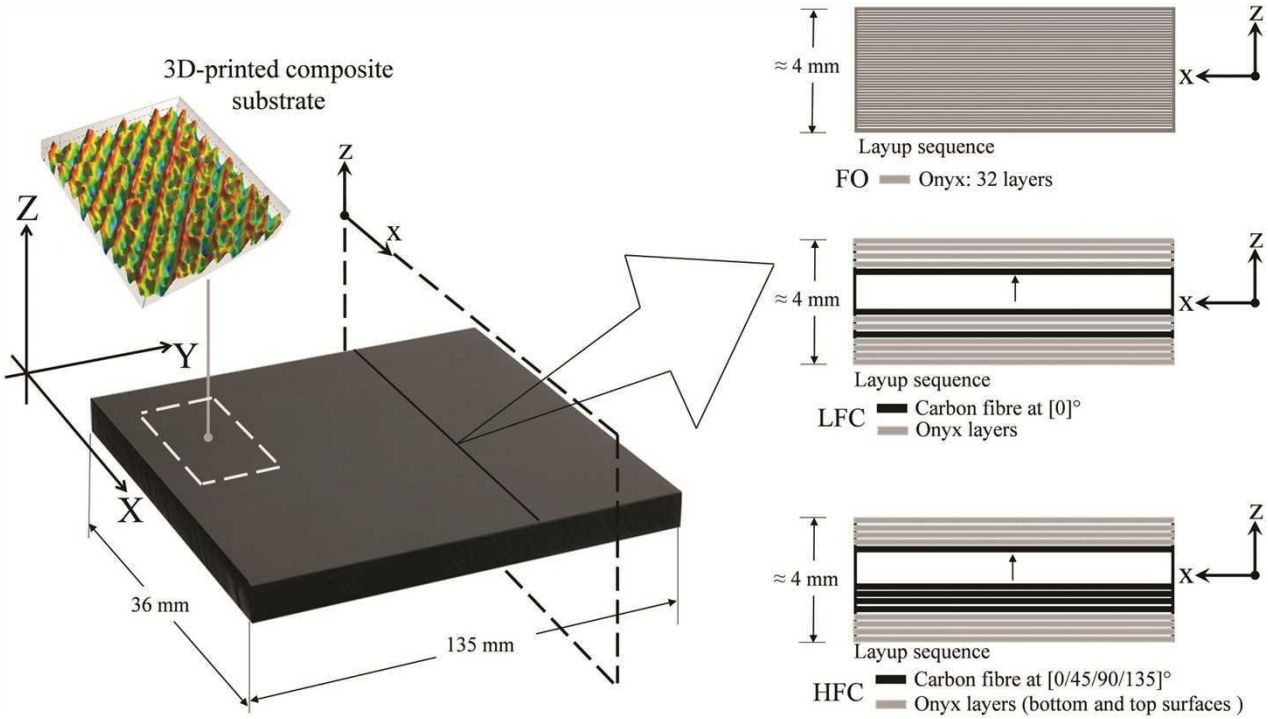

Figure 3. Layup sequences and stratification of 3D-printed composite substrates. (For the clarity of the picture, the layup sequence repetition was not drawn throughout the panel thickness for reinforced laminates).

Printing is performed at 260°C with an estimated speed of 6.90 cm^3/h for the Onyx layers and 2.39 cm^3/h for the carbon fiber layers. For the LFC configuration, the layup sequence "matrix-matrix-reinforcement" was repeated throughout the panel's thickness in its wholeness with a symmetric configuration; the same procedure was applied for the [0/45/90/135]° layup construction. The scan pattern used for the panels' manufacturing is reported in Fig. 2. Concerning the matrix layer, firstly the nozzle defines the boundaries of each layer (the red pattern performed in the x-y plane in Fig. 2) and then the rectangular filler for the matrix core structure. The fiber scan strategy is performed in agreement with the layup sequence defined during the design phase. For the sake of clarity, the fiber scan pattern at 0° only is reported in Fig. 2.

(The experimental data of the panels' manufacturing are summarized in Table 1 pointing out the layup sequence and the strategy of manufacturing, mainly).

The surface finishing of each manufactured panel was observed by means of confocal Leica DCM3D Scan and optical microscopes aiming to analyze the surface characteristics and chose the most appropriate face upon which the deposition can be carried out effectively. An explanatory sketch of the panel stratification and layup is reported in Fig. 3.

A low-pressure CS equipment (Dycomet 423) with nitrogen as a carrier gas was used for the cold spray depositions, which was proved to be the most suitable to successfully spray metal particles on thermoplastic substrates.[28] To limit the cost and the maintenance of the nozzle,[37] a composite nozzle made of a fixed converging-diverging part and an interchangeable divergent part has been used. The geometrical features are summarized in Table 2.

Table 2. Geometrical features of the nozzle.

	Converging-Diverging part			Interchangeable divergent part	
	Inlet section	Throat	Outlet section	Inlet Section	Outlet section
Mean length [mm]	0	7	19	19	139
Mean radius [mm]	4.5	1.25	1.7	2	2.5

Micron-sized powders of pure aluminum (99.9%) were cold-sprayed on the 3D-printed substrates. The processed particles, provided by Toyo Aluminum K.K, have a spherical shape with a mean diameter of about 20 μm; for further details, the cumulative powder distribution (in volume percentage) and the SEM image of the particles are shown in Fig. 4. The choice of particle size and shape was taken by considering what was found in previous studies.[24] The deposition process was computerized by a numerically and remotely controlled pantograph. Under these conditions, the nozzle moves at a set speed and a set standoff distance when spraying onto the substrate.

The strategy adopted for the cold spray deposition on thermoplastic-based polymers was based on preliminary experimental tests as well as literature results.[38] In fact, different coating tracks with a travel speed of the spraying gun equal to 8 mm/s were preliminarily produced by varying the process parameters in a wide range (inlet gas temperature: 150–600°C, inlet gas pressure: 4–8 bar, standoff distance (SoD): 10–80 mm). The abovementioned tests were not here reported for the sake of brevity.

In particular, regarding the inlet gas temperature, the tested values were chosen by taking into account that the temperature of the gas flow on the target surface was below the melting point of the polymeric material. At the same time, the temperature results greater than the glass-transition one; this was done to avoid the deterioration phenomena of the substrate and ensure the softening so that the metallic

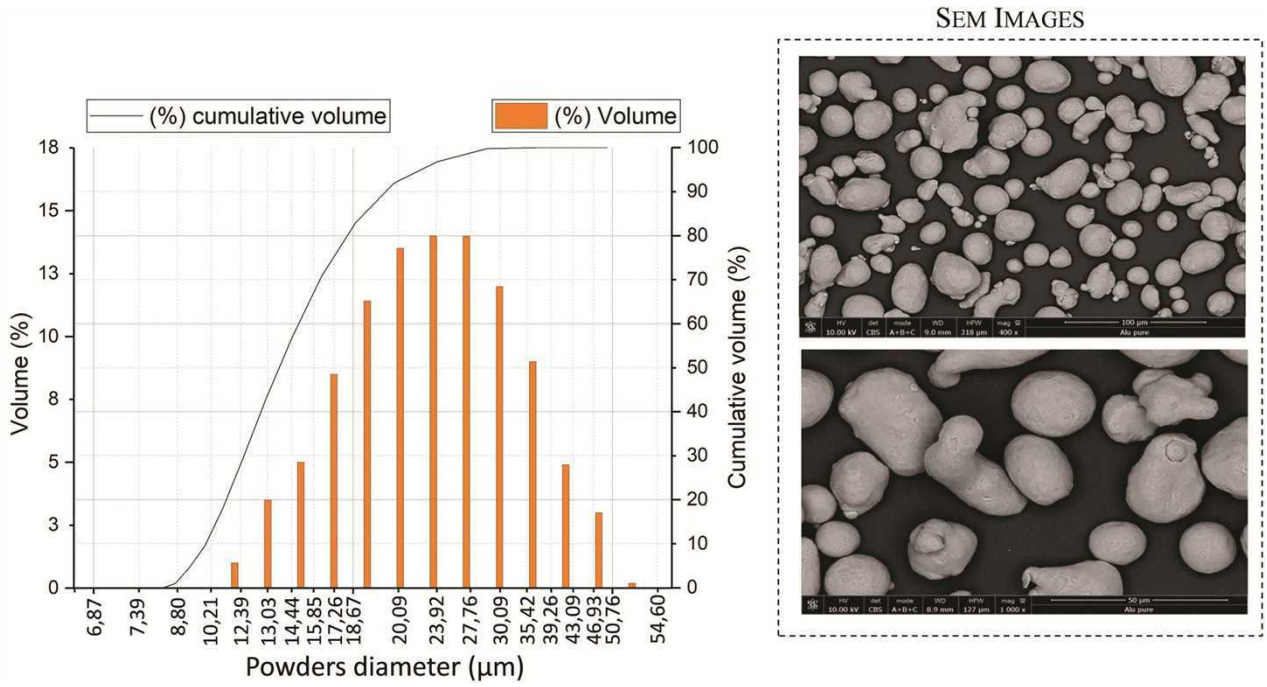

Figure 4. Cumulative powder distribution (in volume percentage) and SEM image of aluminum particles used in this research activity.

Table 3. Combination of CS process parameters used in this research activity.

Panels	Gas Pressure [bar]	SoD [mm]	Gas Temperature [°C]
FO	6	10	250
	6	10	300
	6	10	350
	6	10	400
LFC	6	10	250
	6	10	300
	6	10	350
	6	10	400
HFC	6	10	250
	6	10	300
	6	10	350
	6	10	400

particles can penetrate the polymeric surface. Concerning the gas pressure, the correct value was set considering that the higher the pressure, the higher the substrate erosion due to the strong shot peening effect of the particles. Finally, regarding the standoff distance, the larger the SoD values, the lower the momentum of the particles upon impact with the substrate, resulting in particles rebounding, thus in a poor and thin coating. This result was corroborated by the available literature.[21] In detail, a single-track coating was developed on the surface of each laminate by spraying, layer-by-layer, aluminum particles. The number of passes of the spray gun was set to 3. The inlet gas pressure and the standoff distance were set to 6 bar and 10 mm, respectively, and kept constant during the deposition. Different propellant gas temperatures (250°C, 300°C, 350°C and 400°C) were used to investigate their influence on the deposition of Al powder on each laminate. As summarized in Table 3, 12 different samples are provided with a combination of the above-mentioned parameters.

Microscope observations were carried out on each specimen aiming to analyze the influence of the substrate typology and characteristics on the CS deposition process. For this purpose, samples were cut perpendicularly to the sprayed surface by a precision hacksaw and observed from two different directions: top surface view and cross-section view.

The surface observations were carried out by using a Hitachi TM 3000 SEM and confocal microscope (Leica DCM3D Scan). Optical microscope analyses were also carried out. Aiming to quantify the deposition, the surface coverage and the coating thickness of each coating were calculated similarly to what was done in previous studies.-[37,39–42] As evidenced by Della Gatta et al. work,[39] the amount of the covered surface, indicated as surface coverage, can be considered as an indicator for effective deposition, and, for this purpose, investigations of SEM images have been carried out using the commercial software Image J. To estimate coating heights and roughness measurements, the generation of three-dimensional surfaces of selected coating areas was performed through confocal analyses. After the creation of the surface, results have been exported to LeicaMap Software for the profile extraction. To analyze the morphology of the deposited particles, cross-section analyses were performed. Samples were incorporated in a thermosetting resin by a cold mounting process and then polished and metallized for SEM observations.

Results

Panels' manufacturing

As evidenced in the previous section, three different manufacturing strategies for the PMCs substrates, in terms of layup sequences and fiber density, have been chosen. The results from the optical microscope analyses of the cross-sections of the 3D-printed laminates defined during the design phase are shown in Fig. 5 aiming to better examine the real structures of the panels and correlate them with the deposition outcomes; this was done to point out the relationship between the panel stratification and the CS deposition.

It is possible to notice that both the reinforced panels have four layers of Onyx matrix on the top surface. Four layers of Onyx were also deposited on the bottom surface that is not shown in the figure. In particular, the "matrix-matrix-reinforcement" configuration is certainly visible from Fig. 5 (LFC); regarding the layup sequence of the HFC panel, the lighter phase pointing out from the carbon fiber package is an indicator of the different orientation of the fibers constituting the laminate. Voids and micro defects of the matrix generating between each polymer track and the following one are visible within all the above-mentioned configurations; several studies are carrying out on this topic in the recent literature to optimize the manufacturing process.[43,44]

The results of the confocal microscope observations carried out on both the front and the back faces of a 3D-printed panel are reported in Fig. 6.

In particular, the scope of this preliminary analysis was to study the texturing (namely the random and repetitive deviations from the nominal surface, including roughness, waviness, lay, and flaws) of the target surface and identify the most suitable face to be cold-sprayed.

In Fig. 6, the confocal images of both the faces of the panel FO (Onyx only), chosen as a representative laminate, are shown. More in detail, it can be seen that the front face of the panel is characterized by a more pronounced superficial texturing than the back face. Moreover, the like-grid surface of the former is quite dense with a reduced space between two consecutive valleys of the surface texturing in contrast to what was observed for the back face. The texturing of this last one is characterized by relatively large "isolated dimples" that should not promote the deformation and the sticking of the particles impacting the substrate. When the spacing of the like-grid surface's lines is too high, the presence of the texture should not influence the powder deposition.

Cold spray deposition process

Based on the results presented in the previous section on the different characteristics of the surface texturing resulting from the panels' manufacturing, the powders have been cold-sprayed on the front face of each panel to benefit the effect of the texturing, as shown in Fig. 6.

The effect of the front face texturing of the polymer-based substrate on the cold spray deposition of metallic particles, such as aluminum powder, has been furtherly studied by SEM cross-section observations. In particular, it is possible to note from Fig. 7 that the particles are entirely entangled within

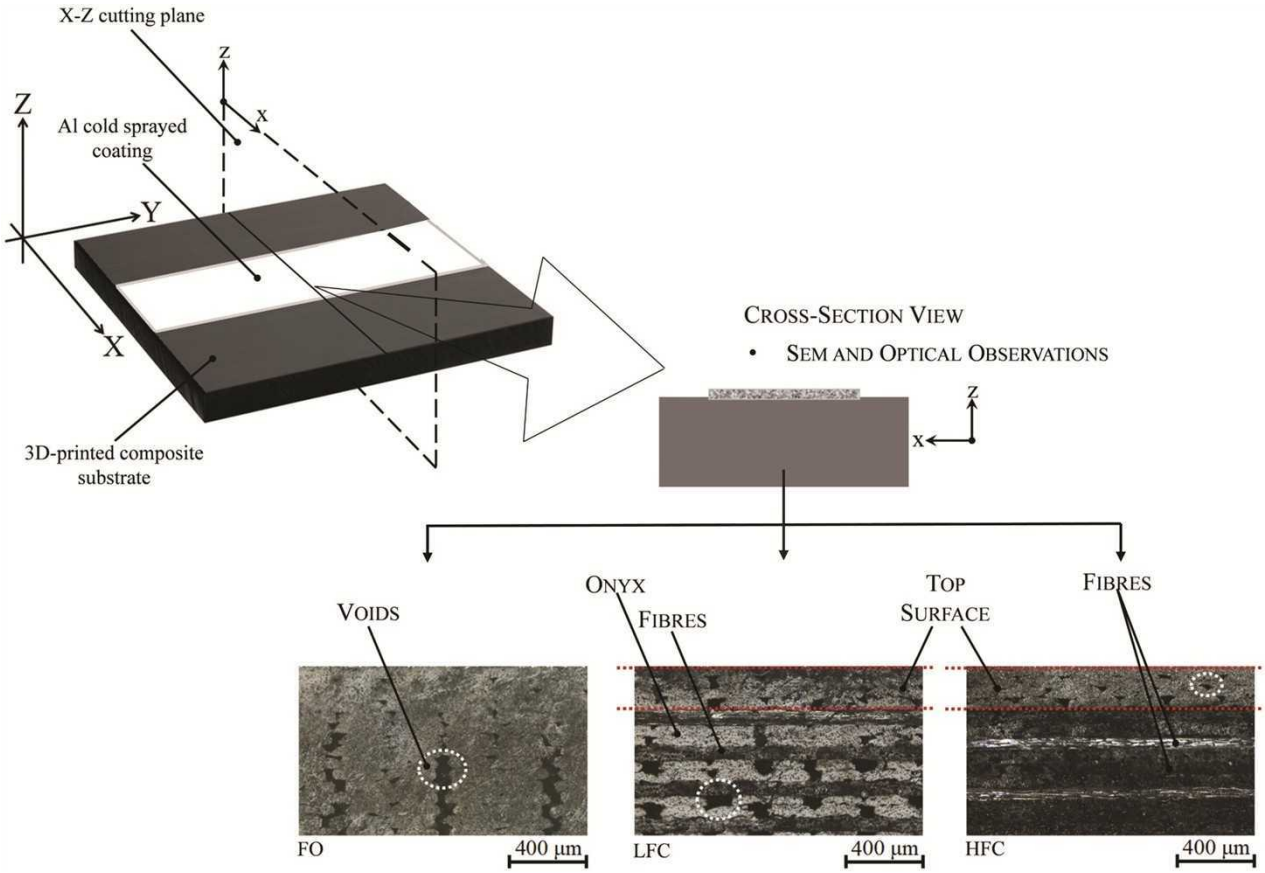

Figure 5. Illustrative sketch and optical images of the layup sequences and stratification of 3D-printed composite substrates. The nomenclature chosen was highlighted in the previous paragraph.

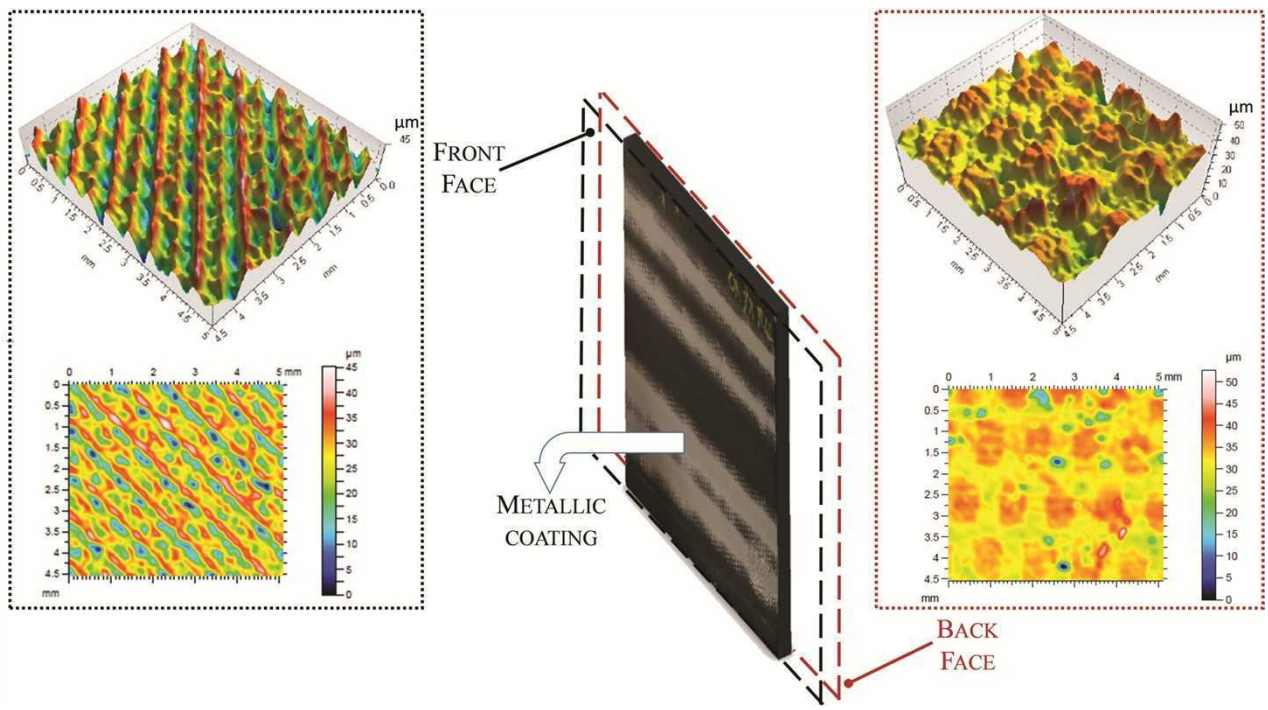

Figure 6. Real picture of 3D-printed laminate (FO configuration) reporting the confocal microscope observations of both the front and the back faces of the panel.

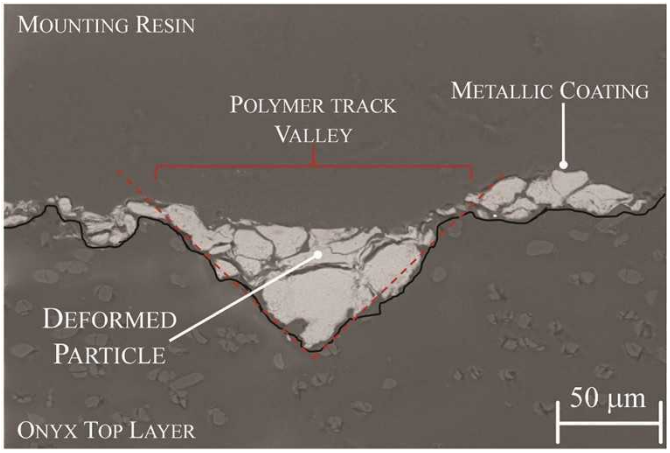

Figure 7. Cross-section SEM image of a coated specimen. The particles are completely locked into the surface texture.

each valley traced by two consecutive polymer tracks and this seems to guarantee an improved adhesion and a relatively high coating thickness and homogeneity. The polymer track valley was highlighted by the red dash-line in Fig. 7.

The macroscopical effects of these phenomena can also be pointed out by observing the top view images of the coated panels. In fact, it is possible to notice from Fig. 8 the presence of metallic bands, made of cold-sprayed aluminum particles, on the surface of the polymeric substrate; this is due to the capacity of the particles to deposit into the portions between two contiguous polymer-based filaments, evidencing the beneficial effect of the surface texturing.

After inspecting the impact of the surface texturing of the specimen on the deposition, namely on the bonding mechanisms involved, it was necessary to highlight the influence of the layup sequence and the strategy of panels' manufacturing. In order to do so, the first parameter the authors analyzed was the surface coverage, which is a good indicator of the number of particles effectively adhered to the substrate.[42] The results obtained for the three typologies of substrates, by varying the gas temperature of CS deposition, are shown in Fig. 9.

It is possible to notice that for all the layup sequences, a rise in the temperature leads to an increment of the surface coverage, reaching values also of about 90% in the coating core.

Regardless of the temperature values analyzed, it is also possible to notice from Fig. 9 that the best performances in terms of surface coverage are guaranteed by the LFC panels (with the layup sequence "matrix-matrix-reinforcement"). This result is also confirmed by SEM observations showing the surface coverage, made of aluminum particles, for each substrate typology (Fig. 10).

It can be seen from Fig. 10b that for the LFC layup sequence, the coating appears denser and more compact than the others with excellent metallic coverage and few voids inside. However, with an increase in the gas temperature, the differences in terms of surface coverage among the three layup sequences tend to smooth out. In fact, it is possible to notice from Fig. 9 that the percentage increase of the surface coverage for LFC panels, for FO and HFC laminates, remains in the relatively

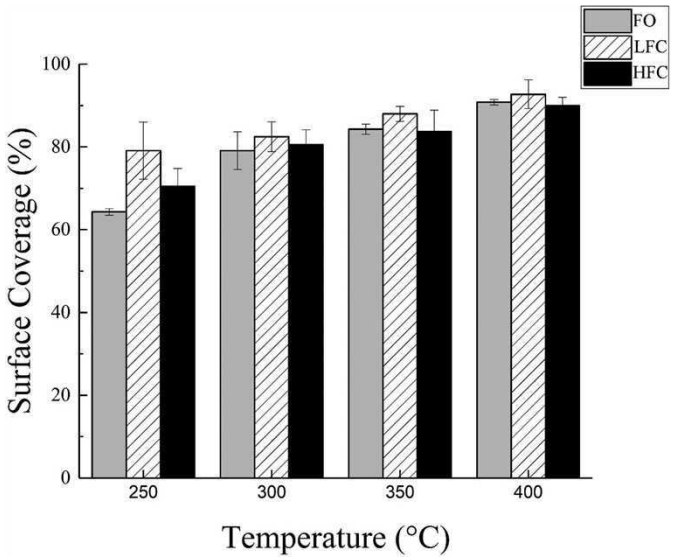

Figure 9. Surface coverage for different substrates and temperatures.

Figure 8. Optical observations of the boundary portion of a coated specimen. The surface texturing is evident with the particles get entangled in the space between two contiguous polymer-based filaments.

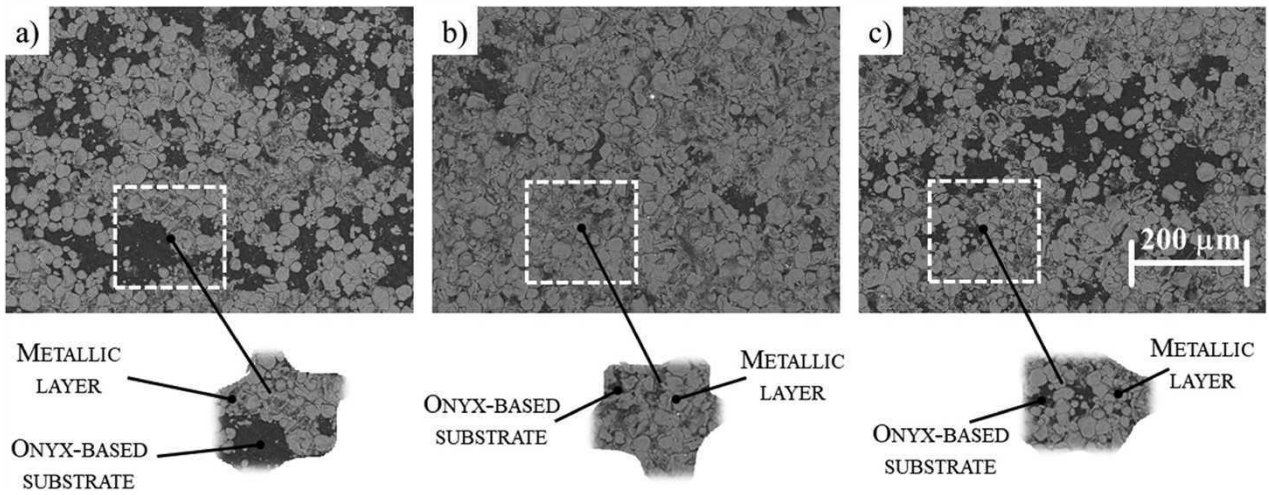

Figure 10. SEM images of the surface of the coatings for the three layup sequences (a) FO, (b) LFC and (c) HFC, respectively. The temperature was set at 250°C.

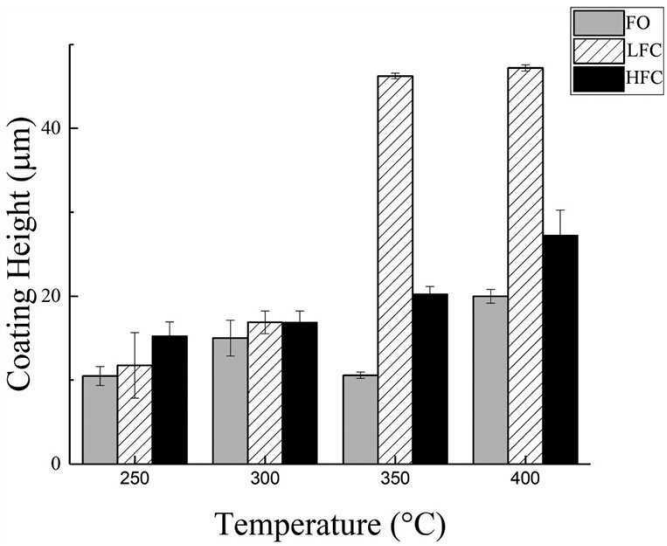

Figure 11. Coating height evaluation for different deposition temperature values on different composite layup sequences.

small range of 2.5% when the temperature of the impinging gas is 400°C, and it seems to be greater than 9% for lower values of the gas temperature, such as 250°C. The main result is that the effects of the manufacturing strategy of the panels tend to be less important with the increase in the gas temperature values.

The coating height analysis furtherly confirms the results obtained for the surface coverage. In particular, it is possible to observe from Fig. 11 that for LFC and HFC panels, an increase in the gas temperature causes an increase in the coating thickness.

Regarding the FO panels, in contrast to what was observed for the other two configuration substrates, there is no appreciable trend of the coating height with the increase in the gas temperature. That means that for every gas temperature value under investigation, the adhesion mechanism involved for this configuration is not influenced more by the cold spray process parameters effectively (such as the gas temperature); the effects of the manufacturing process and layup of the panels seem to have a noticeable influence. In fact, for unreinforced FO panels, it was found that the coating profile follows the morphology of the composite panel surface, meaning that the particles penetrating within the substrate did not firmly anchor with the surrounding surface and did not promote the coating growth.

These results are confirmed by the pictures shown in Fig. 12 reporting a representative roughness profile for each substrate typology.

By looking Fig. 12, it is evident that the manufacturing process of the substrates has a crucial influence on CS deposition with the roughness profile of the coated FO panels that seems to be very similar to the uncoated one. A different behavior was observed for both LFC and HFC panels showing the presence of a thicker coating.

Discussion

Effects of the surface texturing

The texturing of the substrate can have a noticeable influence on CS deposition and the face in contact with the construction plate during the 3D-printing process was proved to be characterized by a smoothed roughness (Fig. 6) that does not promote the sticking of the sprayed particles with the impacted surface. This result was corroborated by literature where the beneficial influence of the superficial texturing has been observed for metal substrates.[45]

Such a result occurring because the powders that impact the space among the grid lines do not feel the presence of the grid itself. Therefore, it seems to be necessary that the valleys of the texturing had a comparable dimension to the feedstock powder diameter; this is a key factor for the particle interlocking between the substrate and the powders as the latter may impinge into the valleys becoming entangled. The superficial texturing characteristics are related to the deposition process of the contiguous Onyx filaments and can be changed by setting the 3D-printing process parameters.

It is known from the literature[21] that the metal coating grow-up on polymer-based surfaces is very difficult, if not impossible, due to energetic phenomena: the anchorage energy between the polymeric substrate and the metallic first layer is

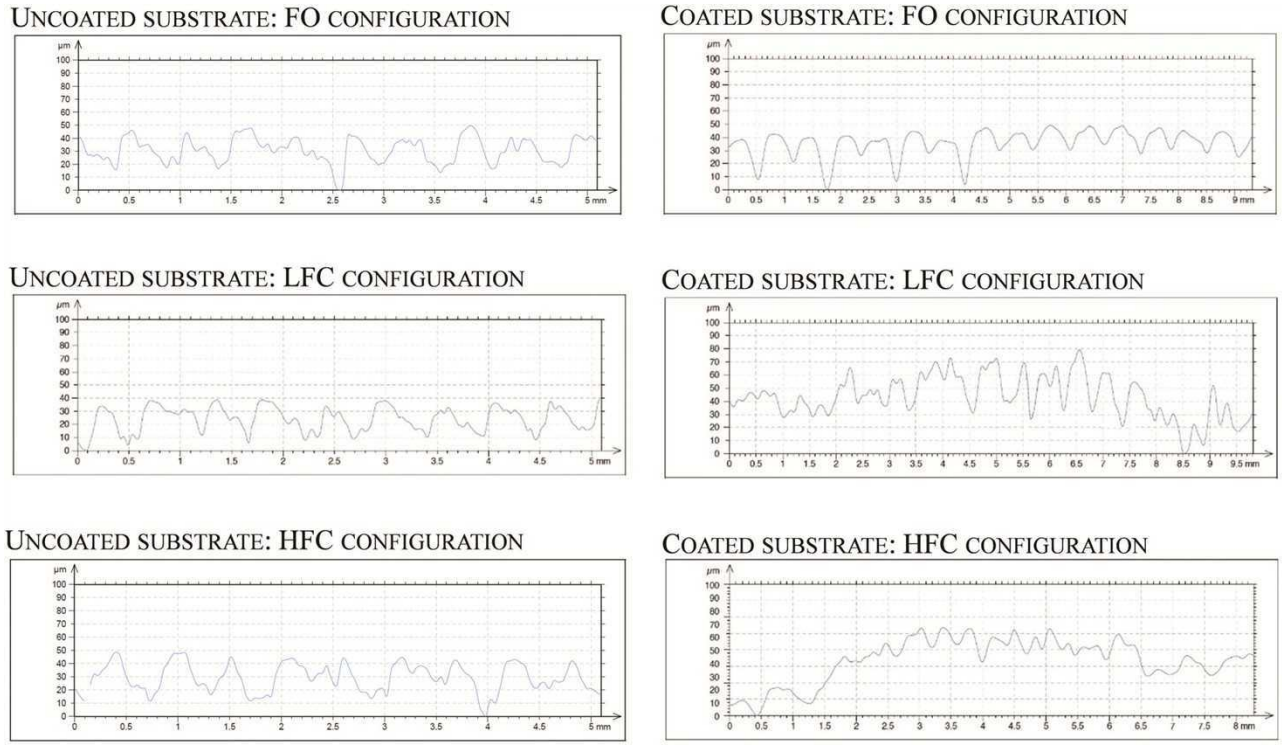

Figure 12. Representative roughness profile of 3D-printed specimens. It is possible to notice that the coating on the FO (full Onyx) panels follows the morphology of the composite panel surface, while in LFC and HFC panels it is not possible to observe the original morphology of the substrate.

smaller than the energy required for the second layer adhering on the first one. The result is that the upcoming particles impacting the first layer remove the "un-bonded particles", so producing erosion and disruption of the coating itself. The front face texturing, in this case, promotes the bonding mechanisms and the interlocking phenomena between the first layer and the substrate with the particles that are well entangled within each valley (see Fig. 7). That means that is very difficult for the upcoming particles to remove them as they remain firmly anchored to the polymer surface, so as they can provide the right energy upon impact the metallic layer, deforming and flattening, so promoting the coating formation and grow-up. These mechanisms prove the effectiveness of the texturing which can be properly defined through the manufacturing route of the panel.

The particle interlocking mechanism was better observed at the boundary area of CSed coating track, where a few particles only possess the right velocity to adhere to the substrate. This intriguing adhesion mechanism is no visible within the core of the coating track due to the relatively high deposition efficiency of the CS process in that area. Moreover, the authors decided to analyze the boundary area also to better understand what are the main mechanisms involved at two contiguous polymer-based filaments during the deposition and, hence, what happens when they overlap during the scan strategy. This analysis could be very useful in the future to plan and design the proper scan strategy for both the CS deposition and the panels' manufacturing.

It is worth noting that the mechanisms that have been observed in Fig. 8 remain valid for all the substrate typologies as the top surface of the panels was obtained with the same filament deposition strategy; the process parameters chosen for the cold spray deposition can influence the number of deposited particles but do not affect the mechanism of adhesion involved and above discussed.

Effects of the panels' manufacturing strategy

The results from Fig. 9 show an increase of the surface coverage values with the gas temperature, regardless of the panels' configuration. The reason is that a rise in gas temperature causes an increase in the mean velocity of the powders[46]; that means that more particles can reach the right velocity to adhere to the substrate, regardless of the layup sequence of the panel. Moreover, an increase in the temperature of the carrier gas leads to the thermal softening of the powders that will deform more when impact the target surface leading to a wider contact area with the substrate and so to better deposition and coverage. Furthermore, the substrate will soften too due to the relatively hotter gas impinging on it: in particular, the softening effect favors the embedding of the particles that firmly anchor with the polymer-based surface. The improvements in the deposition for higher temperatures is furtherly confirmed in the literature.[30]

The best performances of the surface coverage were found for LFC panels, for each value of the investigated gas temperature. This beneficial characteristic may be explained as the LFC panel, compared to the FO panel, is charged with fiber layers, in agreement with the sequence "matrix-matrix-reinforcement"; as proved in literature,[25] the presence of the fibers within the laminate causes the particles to deform more

upon impact, as they collide on a more rigid substrate.[21] A more pronounced deformation of the particles leads to a wider contact area between the particle and the substrates and better bonding. As a consequence, the upcoming particles do not cause erosion and detaching of the first particles deposited that are firmly anchored to the target surface. For this reason, it can be asserted that the deposition window of the fiber-reinforced polymers (like LFC panels) tends to be lower and narrower compared to the pure polymer (like FO panels made of Onyx matrix only): in fact, the particles colliding on a rigid substrate, due to the reinforcement inside, will tend to deform more causing adhesion even for relatively lower velocities. Hence, for a given impact velocity, more particles possess the right velocity to adhere to the substrate for the reinforced LFC panels, so resulting in greater surface coverage values.

As regards the HFC panels, characterized by a higher volume percentage of fibers, it is possible to observe an improvement in terms of surface coverage compared to the full Onyx panel (FO), for the same reasons highlighted above for LFC panels. However, it is possible to notice that the surface coverage of this typology of panels is lower than LFC panels, which are characterized by a lower volume percentage of fibers interspersed with portions of matrix material. The layup sequence of HFC panels causes them to be more rigid than LFC panels. For these reasons, the superficial portion of the matrix cannot deform adequately upon impact, as the fibers constrain its deformation. It is worth noting that four layers of matrix characterize each typology of 3D-printed panels only on the top surface (Fig. 3 for more details). For LFC panels this constraining effect is partially eased by the presence of matrix material layers under every layer of reinforcement (remind the sequence "matrix-matrix-reinforcement"), supporting the deformation of the fibers and allowing for the surface matrix layer to deform more. This mechanism moves up the cold spray deposition window for HFC panels, compared to LFC configuration, due to the greater content of fibers within the composite substrate. In particular, the minimum adhesion velocity increases for the above mentioned reasons as the panel becomes more rigid, as also demonstrated in the literature .[47] From the outcomes above discussed, an optimal value of fiber volume fraction seems to exist. For substrates built using this optimal configuration, the cold spray deposition was proved to give the best results. This further proves that the composite stratification, layup sequence and fiber density, which are strictly related to the composite manufacturing processes, have a noticeable influence on the CS deposition process.

At the same time, the maximum velocity for the adhesion to occur (the erosion velocity) tends to become lower for both LFC and HFC panels. Because of the excessively high velocities, the particles tend to erode the substrate easily as the polymer cannot deform rapidly enough at such high velocities, as the fibers tend to constrain it. It is evident that this phenomenon is more pronounced for HFC panels. An explanatory sketch of the effects of the panels manufacturing and layup construction on the cold spray deposition window is reported in Fig. 13.

It is worth noting that the above mentioned considerations remain valid for each temperature value of the carrier gas. However, when the relatively hotter gas carrying the particles impinges the reinforced substrate, the thermal softening effects of the material become more important so that the constraining phenomena produced by the fibers are released without noticeable stiffening effects for the polymeric substrate. At relatively higher temperatures of the gas, the softened polymer matrix can flow more freely and deform upon impact.[29] The result is that the powders, under these gas conditions, impact a less rigid surface because the contribution of the fibers to the stiffening of the panels is less prominent and does not produce severe deformation of the particles resulting in a lower increment of the metallic coverage compared to the unreinforced panels.

As a result of these considerations, it can be asserted that the presence of the fibers has a beneficial effect on particle adhesion. However, a limit fiber content/fiber-layer thickness value exists, upon which the beneficial effect of the reinforcement is nullified and an overall lowering of the properties in terms of adhered particles is observed.

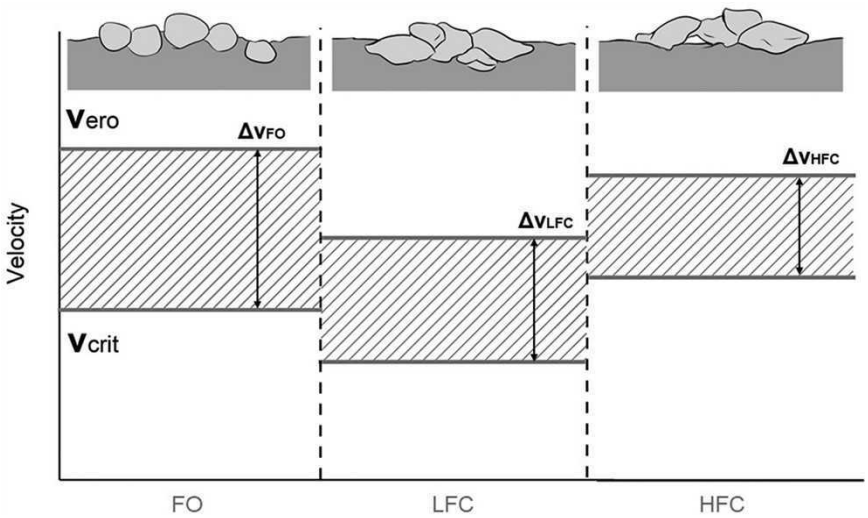

Figure 13. Illustrative sketch of deposition windows for three different typologies of substrates. The deposition window of both LFC (ΔV_{LFC}) and HFC (ΔV_{HFC}) panels tend to be lower and narrower compared to that of FO (ΔV_{FO}) panels: $\Delta V_{FO} > \Delta V_{LFC} > \Delta V_{HFC}$.

The results obtained from the surface coverage analyses were also confirmed by the coating height graphs (namely, with the increase of the gas temperature, more particles can reach the right velocity to adhere and the thermal softening effects become successfully for deposition[48]). However, the difference in trend observed for FO panels is related to the increased penetration of the particles within the unreinforced polymeric matrix that is more evident in the FO panels, being the substrate less rigid than the reinforced LFC and HFC panels. As proved by the relatively low values of the surface coverage from the analysis above discussed, for FO panels the particles seem to not fully adhere to the substrate and are carried off from the impinging particles hindering the coating growth. This phenomenon takes place also at relatively higher temperature values of the carrier gas as the particles further penetrate the softened target surface. That is the reason for which the coating height is the lowest for FO panels.

Moreover, for FO laminates, the relatively soft surface seems to not cause severe deformation of the impacting powders, so resulting in a poor adhered metallic layer tending to be removed from the upcoming particles.[28] It follows that, for this kind of sample, the coating grow-up is very difficult and the coating was proved to track the morphology of the panel surface with visible peaks and valleys of the coating profile (see Fig. 12). Hence, the coating height is strongly affected by the morphology of the substrate, which in turn depends on the manufacturing strategy adopted. In fact, it was proved that this phenomenon seems to be not so prominent for the reinforced panels (for both LFC and HFC laminates) that show an appreciable coating profile highlighting the ability of the particles to form a thicker metallic coating.

All the results found in this activity prove that the bonding mechanisms involved depend on the substrate typology, the substrate scan strategy and the layup sequence. In fact, the beneficial effects of the fibers within the laminates were also confirmed by the results above.

It is evident that the 3D-printing manufacturing process for the composite laminates represents a potential solution for the customization of the panels that should be produced to fit better the CS deposition requirements.

Conclusions

The aim of this research work was to develop a novel manufacturing route of integrated 3D-printed composites and cold-sprayed metallic layer in order to obtain tailored hybrid constructions with enhanced properties. For this purpose, both the layup sequence and stratification of the composite substrates and the cold spray process parameters were varied to study the fabrication process in its wholeness. Therefore, based on the experimental results presented and discussed in the previous sections, the following conclusions could be drawn:

- The integrated manufacturing solution here developed involving the FFF technology and the cold spray technique for the production of tailored composite structures was proved to be effective.
- The effects of the surface texturing of the 3D-printed panels on CS deposition were proved: the distance among the valleys of the texturing should have a comparable dimension to the feedstock powder diameter. The best results of depositions were obtained when the like-grid surface's lines is in the range of 100 μm. Higher values of distance do not promote the particle deformation and adhesion.
- The best values of the surface coverage were found for LFC panels and for the highest value of the gas temperature investigated (T = 400°C). This is due to a larger number of particles reaching the right velocity to adhere and the thermal softening effects experienced by the substrates. The difference in the surface coverage values among the three layup configurations was found to be maximum (greater than 9%) for the lowest value of the gas temperature (250°C). For this condition, the panels' manufacturing strategy becomes more important.
- The coating height was proved to increase with the gas temperature and it reached the highest values (≈45 μm) for LFC panels metallized with a gas temperature equal to 400°C. For FO panels the coating height did not show this trend as the particles impact on a less rigid surface that does not promote the coating buildup. This proves the beneficial effects of the fibers within the laminate on the CS deposition process.
- A threshold fiber content/fiber-layer thickness value was proved to exist, upon which the beneficial effect of the reinforcement is nullified and an overall lowering of the properties in terms of surface coverage and coating height is observed.

Based on the results obtained, it can be asserted that the 3D-printing process represents a very promising and potential solution for the manufacturing of the composite structures to be used as substrates for the cold spray deposition; in this regard, a more detailed study based on the influence of the panels' manufacturing strategy and the fiber volume density of the composites will be planned by the authors, aiming to better understand the effects of these parameters on the 3D-integrated process.

Acknowledgments

The authors want to acknowledge the Italian Ministry for University and Research for funding the research activity through the research grant "COSMEC" (2017N4422T), within the PRIN 2017 framework.

Funding

This work was supported by the COSMEC [2017N4422T].

ORCID

Roberta Della Gatta http://orcid.org/0000-0002-3398-8970
Francesco Delloro http://orcid.org/0000-0002-3068-180X
Antonello Astarita http://orcid.org/0000-0003-3214-3375

References

[1] Kulkarni, P.; Mali, K. D.; Singh, S. An Overview of the Formation of Fibre Waviness and Its Effect on the Mechanical Performance of Fibre Reinforced Polymer Composites. *Compos. Part A Appl. Sci. Manuf.* 2020, *137*, 106013. DOI: 10.1016/j.compositesa.2020.106013.

[2] Hale, D. K.;. The Physical Properties of Composite Materials. *J. Mater. Sci.* 1976, *11*(11), 2105–2141. DOI: 10.1007/PL00020339.

[3] Miao, J.; Fang, Y.; Yang, X.; Zhu, Y.; Hu, A.; Wang, G. Fabrication, Flame Retardancy and Physical Properties of Phosphorus Containing Porous Organic Polymers/epoxy Resin Composites. *Polym. Degrad. Stab.* 2020, *176*, 109159. DOI: 10.1016/j.polymdegradstab.2020.109159.

[4] Jin, S.; Liu, Z.; Qian, L.; Qiu, Y.; Chen, Y.; Xu, B. Epoxy Thermoset with Enhanced Flame Retardancy and Physical-mechanical Properties Based on Reactive Phosphaphenanthrene Compound. *Polym. Degrad. Stab.* 2020, *172*, 109063. DOI: 10.1016/j.polymdegradstab.2019.109063.

[5] Li, J.; Ai, Z.; Zhang, L. Design of a Neutral electro-Fenton System with Fe@Fe2O3/ACF Composite Cathode for Wastewater Treatment. *J. Hazard. Mater.* 2009, *164*(1), 18–25. DOI: 10.1016/j.jhazmat.2008.07.109.

[6] Straumal, B. B.; Vershinin, N. F.; Cantarero-Saez, A.; Friesel, M.; Zieba, P.; Gust, W. Vacuum Arc Deposition of Protective Layers on Glass and Polymer Substrates. *Thin Solid Films*. 2001, *383*(1–2), 224–226. DOI: 10.1016/S0040-6090(00)01799-5.

[7] Zhou, Q.; Chen, H.; Wang, Y. Region-selective Electroless Gold Plating on Polycarbonate Sheets by UV-patterning in Combination with Silver Activating. *Electrochim. Acta*. 2010, *55*(7), 2542–2549. DOI: 10.1016/j.electacta.2009.12.024.

[8] Mekaru, H.; Koizumi, O.; Ueno, A.; Takahashi, M. Guide Structure with Pole Arrays Imprinted on Nylon Fiber. *Microelectron. Eng.* 2010, *87*(5–8), 922–926. DOI: 10.1016/j.mee.2009.11.174.

[9] Robitaille, F.; Yandouzi, M.; Hind, S.; Jodoin, B. Metallic Coating of Aerospace Carbon/epoxy Composites by the Pulsed Gas Dynamic Spraying Process. *Surf. Coatings Technol.* 2009, *203*(19), 2954–2960. DOI: 10.1016/j.surfcoat.2009.03.011.

[10] Zhou, X. L.; Chen, A. F.; Liu, J. C.; Wu, X. K.; Zhang, J. S. Preparation of Metallic Coatings on Polymer Matrix Composites by Cold Spray. *Surf. Coatings Technol.* 2011, *206*(1), 132–136. DOI: 10.1016/j.surfcoat.2011.07.005.

[11] Lupoi, R.; O'Neill, W. Deposition of Metallic Coatings on Polymer Surfaces Using Cold Spray. *Surf. Coatings Technol.* 2010, *205*(7), 2167–2173. DOI: 10.1016/j.surfcoat.2010.08.128.

[12] Rokni, M. R.; Feng, P.; Widener, C. A.; Nutt, S. R. Depositing Al-Based Metallic Coatings onto Polymer Substrates by Cold Spray. *J. Therm. Spray. Technol.* 2019, *28*(7), 1699–1708. DOI: 10.1007/s11666-019-00911-y.

[13] Schmidt, T.; Assadi, H.; Gärtner, F.; Richter, H.; Stoltenhoff, T.; Kreye, H.; Klassen, T. From Particle Acceleration to Impact and Bonding in Cold Spraying. *J. Therm. Spray. Technol.* 2009, *18*(5–6), 794–808. DOI: 10.1007/s11666-009-9357-7.

[14] Schmidt, T.; Gärtner, F.; Assadi, H.; Kreye, H. Development of a Generalized Parameter Window for Cold Spray Deposition. *Acta Mater.* 2006, *54*(3), 729–742. DOI: 10.1016/j.actamat.2005.10.005.

[15] Che, H.; Vo, P.; Yue, S. Metallization of Carbon Fibre Reinforced Polymers by Cold Spray. *Surf. Coatings Technol.* 2017, *313*, 236–247. DOI: 10.1016/j.surfcoat.2017.01.083.

[16] Che, H.; Vo, P.; Yue, S. Investigation of Cold Spray on Polymers by Single Particle Impact Experiments. *J. Therm. Spray. Technol.* 2018, 1–9. DOI: 10.1007/s11666-018-0801-4.

[17] Moridi, A.; Hassani-Gangaraj, S. M.; Guagliano, M.; Dao, M. Cold Spray Coating: Review of Material Systems and Future Perspectives. *Surf. Eng.* 2014, *30*, 369–395. DOI: 10.1179/1743294414Y.0000000270.

[18] Dykhuizen, R. C.; Smith, M. F.; Gilmore, D. L.; Neiser, R. A.; Jiang, X.; Sampath, S. Impact of High Velocity Cold Spray Particles. *J. Therm. Spray. Technol.* 1999, *8*(4), 559–564. DOI: 10.1361/105996399770350250.

[19] Raletz, F.; Vardelle, M.; Ezo'o, G. Critical Particle Velocity under Cold Spray Conditions. *Surf. Coatings Technol.* 2006, *201*(5), 1942–1947. DOI: 10.1016/j.surfcoat.2006.04.061.

[20] Assadi, H.; Gärtner, F.; Stoltenhoff, T.; Kreye, H. Bonding Mechanism in Cold Gas Spraying. *Acta Mater.* 2003, *51*(15), 4379–4394. DOI: 10.1016/S1359-6454(03)00274-X.

[21] Che, H.; Chu, X.; Vo, P.; Yue, S. Metallization of Various Polymers by Cold Spray. *J. Therm. Spray. Technol.* 2018, *27*(1–2), 169–178. DOI: 10.1007/s11666-017-0663-1.

[22] Ganesan, A.; Affi, J.; Yamada, M.; Fukumoto, M. *Bonding behavior studies of cold sprayed copper coating on the PVC polymer substrate*. vol. 207. 2012.

[23] Pattison, J.; Celotto, S.; Khan, A.; O'Neill, W. Standoff Distance and Bow Shock Phenomena in the Cold Spray Process. *Surf. Coatings Technol.* 2008, *202*(8), 1443–1454. DOI: 10.1016/j.surfcoat.2007.06.065.

[24] Jeandin, M.; Rolland, G.; Descurninges, L. L.; Berger, M. H. Which Powders for Cold Spray? *Surf. Eng.* 2014, *30*(5), 291–298. DOI: 10.1179/1743294414Y.0000000253.

[25] Gillet, V.; Aubignat, E.; Costil, S.; Courant, B.; Langlade, C.; Casari, P.; Knapp, W.; Planche, M. P. Development of Low Pressure Cold Sprayed Copper Coatings on Carbon Fiber Reinforced Polymer (CFRP). *Surf. Coatings Technol.* 2019, *364*, 306–316. DOI: 10.1016/j.surfcoat.2019.01.011.

[26] Perna, A. S.; Viscusi, A.; Astarita, A.; Boccarusso, L.; Caraviello, A.; Carrino, L.; Durante, M.; Sansone, R. Experimental Study of Functionalized Polymer Matrix Composite with Multi-Material Metal Coatings Produced by Means of Cold Spray Technology. *Key Eng. Mater.* 2019, *813*, 267–272. DOI: 10.4028/www.scientific.net/KEM.813.267.

[27] Viscusi, A.; Antonucci, V.; Carrino, L.; Della Gatta, R.; Lopresto, V.; Papa, I.; Perna, A. S.; Ricciardi, M. R.; Astarita, A. Manufacturing of an Innovative Composite Structure: Design, Manufacturing and Impact Behaviour. *Compos. Struct.* 2020, *250*, 112637. DOI: 10.1016/j.compstruct.2020.112637.

[28] Ganesan, A.; Yamada, M.; Fukumoto, M. Cold Spray Coating Deposition Mechanism on the Thermoplastic and Thermosetting Polymer Substrates. *J. Therm. Spray. Technol.* 2013, *22*(8), 1275–1282. DOI: 10.1007/s11666-013-9984-x.

[29] Varinor, G. D.; Guipont, V.; Giraud, D.; Borit, F.; Guipont, V.; Jeandin, M.; Malhaire, J. M. *Metallization of a polymer using cold spray: Application to aluminum coating of polyamide 66 Characterization and modeling of coating properties and microstructure evolution View project Metallization of a Polymer Using Cold Spray: Application to Aluminum*. 2012.

[30] Bortolussi, V.; Borit, F.; Chesnaud, A.; Jeandin, M.; Faessel, M.; Figliuzzi, B.; Willot, F.; Roche, K.; Surdon, G. *Cold spray of metal-polymer composite coatings onto carbon fiber-reinforced polymer (CFRP)*. 7. 2016.

[31] K., P.; M., M.; P., S. P. P. S.P. Technologies in Additive Manufacturing for Fiber Reinforced Composite Materials: A Review. *Curr. Opin. Chem. Eng.* 2020, *28*, 51–59. DOI: 10.1016/j.coche.2020.01.001.

[32] Zindani, D.; Kumar, K. An Insight into Additive Manufacturing of Fiber Reinforced Polymer Composite. *Int. J. Light. Mater. Manuf.* 2019, 267–278. DOI: 10.1016/j.ijlmm.2019.08.004.

[33] Das, A.; Chatham, C. A.; Fallon, J. J.; Zawaski, C. E.; Gilmer, E. L.; Williams, C. B.; Bortner, M. J. Current Understanding and Challenges in High Temperature Additive Manufacturing of Engineering Thermoplastic Polymers. *Addit. Manuf.* 2020, 101218. DOI: 10.1016/j.addma.2020.101218.

[34] Brenken, B.; Barocio, E.; Favaloro, A.; Kunc, V.; Pipes, R. B. Fused Filament Fabrication of Fiber-reinforced Polymers: A Review. *Addit. Manuf.* 2018, 1–16. DOI: 10.1016/j.addma.2018.01.002.

[35] Blok, L. G.; Longana, M. L.; Yu, H.; Woods, B. K. S. An Investigation into 3D Printing of Fibre Reinforced Thermoplastic Composites. *Addit. Manuf.* 2018, *22*(November2017), 176–186. DOI: 10.1016/j.addma.2018.04.039.

[36] Kabir, S. M. F.; Mathur, K.; Seyam, A.-F. M. A Critical Review on 3D Printed Continuous Fiber-reinforced Composites: History,

Mechanism, Materials and Properties. *Compos. Struct.* 2020, *232*, 111476. DOI: 10.1016/j.compstruct.2019.111476.

[37] Della Gatta, R.; Viscusi, A.; Perna, A. S.; Caraviello, A.; Astarita, A. Feasibility of Steel Powder Deposition on Composites through Cold Spray. *Mater. Manuf. Process.* 2020, *1–11*. DOI: 10.1080/10426914.2020.1832693.

[38] Gonzalez, R.; Ashrafizadeh, H.; Lopera, A.; Mertiny, P.; McDonald, A. A. Review of Thermal Spray Metallization of Polymer-Based Structures. *J. Therm. Spray Technol.* 2016, *25*, 897–919. DOI: 10.1007/s11666-016-0415-7.

[39] Della Gatta, R.; Viscusi, A.; Perna, A. S.; Caraviello, A.; Astarita, A. Cold Spray Process for the Production of AlSi10Mg Coatings on Glass Fibers Reinforced Polymers. *Mater. Manuf. Process.* 2020, 1–16. DOI: 10.1080/10426914.2020.1813895.

[40] Małachowska, A.; Winnicki, M.; Stachowicz, M.; Korzeniowski, M. Metallisation of Polycarbonates Using a Low Pressure Cold Spray Method. *Surf. Eng.* 2018, *34*(3), 251–258. DOI: 10.1080/02670844.2016.1277843.

[41] Vucko, M. J.; King, P. C.; Poole, A. J.; Carl, C.; Jahedi, M. Z.; De Nys, R. Cold Spray Metal Embedment: An Innovative Antifouling Technology. *Biofouling.* 2012, *28*(3), 239–248. DOI: 10.1080/08927014.2012.670849.

[42] Lupoi, R.; Stenson, C.; McDonnell, K. A.; Dowling, D. P.; Ahearne, E. Antifouling Coatings Made with Cold Spray onto Polymers: Process Characterization. *CIRP Ann.* 2016, *65*(1), 545–548. DOI: 10.1016/j.cirp.2016.04.015.

[43] González-Estrada, O. A.; Pertuz, A.; Quiroga, J. *Evaluation of Tensile Properties and Damage of Continuous Fibre Reinforced 3D-printed Parts. Key Engineering Materials*. 2018; Trans Tech Publications Ltd: Switzerland. Vol. 774 KEM. 161–166.

[44] Bárnik, F.; Vaško, M.; Sága, M.; Handrik, M.; Sapietová, A.; Malujda, I.; Dudziak, M.; Krawiec, P.; Talaśka, K.; Wilczyński, D. Mechanical Properties of Structures Produced by 3D Printing from Composite Materials. *MATEC Web Conf.* 2019, *254*, 01018. DOI: 10.1051/matecconf/201925401018.

[45] Viscusi, A.; Astarita, A.; Genna, S.; Leone, C. On the Influence of Different Superficial Laser Texturing on the Deposition of Powders through Cold Spray Process. *Trans. Inst. Met. Finish.* 2018, *96*(1), 34–40. DOI: 10.1080/00202967.2018.1403096.

[46] Prisco, U.;. Size-dependent Distributions of Particle Velocity and Temperature at Impact in the Cold-gas Dynamic-spray Process. *J. Mater. Process. Technol.* 2015, *216*, 302–314. DOI: 10.1016/j.jmatprotec.2014.09.013.

[47] Kalsi, S. S.; Sidhu, T. S.; Singh, H.; Karthikeyan, J. Behavior of Cold Spray Coating in Real Incineration Environment. *Mater. Manuf. Process.* 2016, *31*(11), 1468–1475. DOI: 10.1080/10426914.2014.912319.

[48] Trexler, M. D.; Carter, R.; De Rosset, W. S.; Gray, D.; Helfritch, D. J.; Champagne, V. K. Cold Spray Fabrication of Refractory Materials for Gun Barrel Liner Applications. *Mater. Manuf. Process.* 2012, *27*(8), 820–824. DOI: 10.1080/10426914.2011.648690.